

# The importance of longer wavelength reheating in dual-pulse laser-induced breakdown spectroscopy

R.W. Coons · S.S. Harilal · S.M. Hassan · A. Hassanein

Received: 13 September 2011 / Revised version: 6 March 2012 / Published online: 21 April 2012  
© Springer-Verlag 2012

**Abstract** Dual-pulse laser-induced breakdown spectroscopy (LIBS) provides improved sensitivity compared to conventional single-pulse LIBS. We used a combination of Nd:yttrium aluminum garnet (YAG) and CO<sub>2</sub> lasers to improve the sensitivity of LIBS. Significant emission intensity enhancement is noticed for both excited neutral lines and ionic lines for dual-pulse LIBS compared to single-pulse LIBS. However, the enhancement factor is found to be dependent on the energy levels of the lines, and resonance lines provided maximum enhancement. Our results indicate that IR reheating will cause significant improvement in sensitivity, regardless of the conditions, even with an unfocused reheating beam. The improved sensitivity with a YAG-CO<sub>2</sub> laser combination is caused by the effective reheating of the preplume with a longer wavelength laser is due to efficient inverse Bremsstrahlung absorption. The role of the spot sizes, inter-pulse delay times, energies of the preheating and reheating pulses on the LIBS sensitivity improvements are discussed.

## 1 Introduction

Laser-induced breakdown spectroscopy (LIBS) provides multi-elemental in-situ sample analysis down to trace con-

centrations for many elements, including most light elements (H, C, O, N). Hence, LIBS is a common and effective technique for chemical fingerprinting and elemental analysis, where an intense laser is focused onto a target material, which is then ablated and excited into a plasma state [1]. By focusing the beam upon a distant target, LIBS can serve as the basis of a remote detection system for security applications [2, 3]. Laser plasmas exist in the form of brief sparks, which must be close to a light collector system in order to provide usable signals. The LIBS technique is also used for detecting airborne biological agents, quantitative analysis of aerosols, etc. [1].

Although LIBS is suited for various applications, this technique possesses a lower sensitivity and precision than the other forms of elemental analysis, such as inductively coupled-plasma mass-spectrometry (ICP-MS). Currently, there is much research being conducted on techniques to improve the sensitivity of LIBS or to increase the spectral intensity, to compensate for signal degradation over stand-off differences [2, 3]. One technique for doing so is dual-pulse LIBS (DP-LIBS), where laser plasmas are reheated shortly after their formation with a second laser pulse [4]. Previous dual-pulse studies, which utilized Nd:YAG lasers and their harmonics for both plasma formation and reheating, showed a signal enhancement factor of 2–12× [4, 5]. However, the reasons for the increased sensitivity have not been yet univocally ascertained, and a little effort has been made to understand the physics behind this emission enhancement. Some of the explanations given for signal enhancement include a higher mass ablation [6–9], a larger plasma volume [8], the reheating of the plume [9, 10], the lowering of the laser shielding effect [6], the heating of the target by the first pulse and the reduction in ambient density [11] preconditioning [12, 13] or rekindling of the plume [14], and the confinement of the new plume by the

---

R.W. Coons (✉) · S.S. Harilal · S.M. Hassan · A. Hassanein  
School of Nuclear Engineering, and Center for Materials Under  
Extreme Environment, Purdue University, West Lafayette,  
IN 47907, USA  
e-mail: [ryancoonsyhg@gmail.com](mailto:ryancoonsyhg@gmail.com)

S.S. Harilal  
e-mail: [hari@purdue.edu](mailto:hari@purdue.edu)

A. Hassanein  
e-mail: [hassanein@purdue.edu](mailto:hassanein@purdue.edu)

first shock wave boundaries [15], etc. Recently, it has been demonstrated that IR laser reheating provides significant improvement in LIBS [4].

The use of shorter wavelengths for LIBS offers higher photon energies to drive ionization and bond breaking processes, and to induce secondary effects, such as photonization and non-thermal ablation mechanisms, and inverse Bremsstrahlung becomes a less important process [16]. The use of UV lasers for LIBS also has the added advantage of a shorter optical penetration depth, which provides greater laser energy per unit volume for ablation [16]. In general, shorter laser wavelengths provide higher ablation rates which are easier to control and reproduce, with a lower fluence needed to initiate ablation [16], and a lower elemental fractionation in laser-ablation ICP-MS [17]. The longer wavelengths provide more heating of the plume through inverse Bremsstrahlung, but with a lower ablation rate [18–20]. Hence, it is better to use a sequence of short and long wavelength lasers for DP-LIBS as pre-pulsing and reheating beams.

In this paper, we investigated the role of 10.6  $\mu\text{m}$  reheating of a LIBS plume generated by 1.06  $\mu\text{m}$  laser. DP-LIBS spectral intensity depends on several experimental parameters, and some of these are pump and reheating spot sizes and pulse energies, inter-pulse delay, data integration time and delay with plasma formation. We have explored the signal enhancement in DP-LIBS in five discrete experiments with varying laser spot sizes, energies, and delay times, from which the signal enhancement is calculated as a function of time. In addition, the electron temperature and densities of the LIBS plasma are estimated using optical emission spectroscopy to identify the reasons for signal enhancement.

## 2 Experimental setup

A schematic of the experimental setup is given in Fig. 1. Plasmas were generated from 1.06  $\mu\text{m}$ , 6 ns full width half maximum (FWHM) pulses from a Nd:YAG laser. The YAG laser was attenuated using a combination of a half-wave plate and a polarizing cube. The LIBS plume generated by the YAG laser was reheated with a transversally excited atmosphere (TEA) CO<sub>2</sub> laser, operating at 10.6  $\mu\text{m}$ . These CO<sub>2</sub> laser pulses consisted of a 45–50 ns FWHM pulse followed by a weak nitrogen tail, which lasts over a few  $\mu\text{s}$  (see Fig. 1). These laser pulses excite sheets of commercial-grade Al mounted to a servo-motor controlled XYZ translation stage. The XYZ stage allows target translation between shots to provide a fresh target surface for each trial, to mitigate effects caused by target drilling and crater formation. All experiments were conducted at ambient atmospheric conditions. Both the pre-plume and reheating laser pulses were aligned to coincide on a single point. The YAG laser was

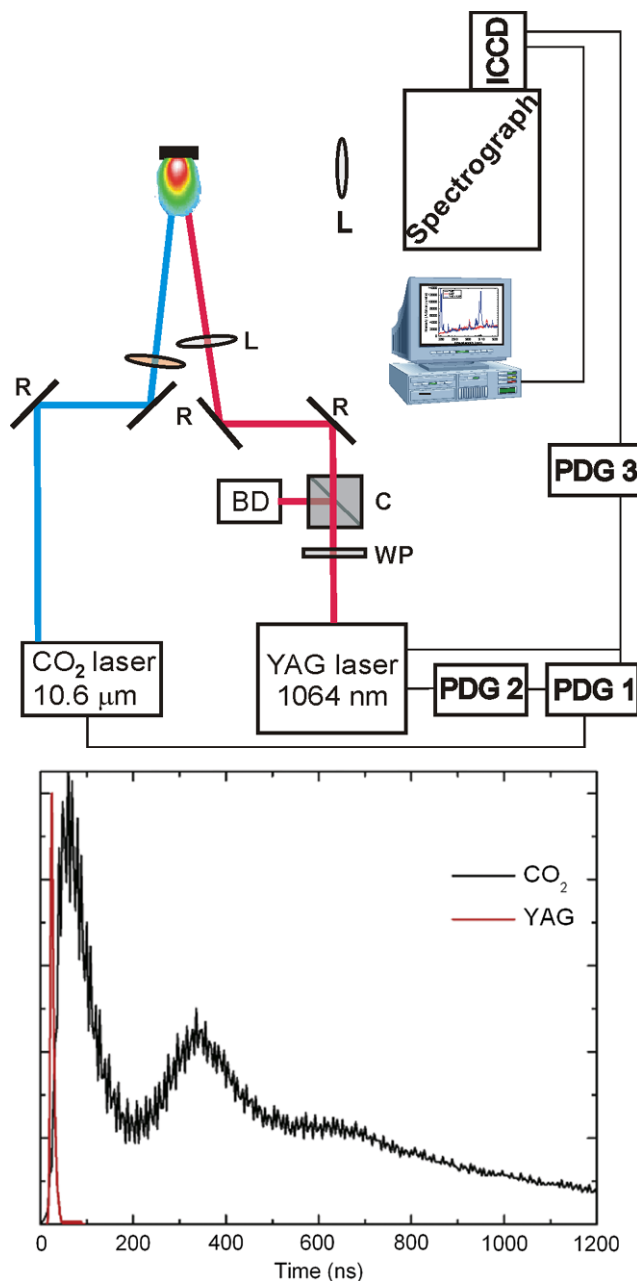


**Fig. 1** Schematic of the dual-pulse LIBS setup (*top*) and typical temporal profiles of the pre-pulse and the reheating pulse (*bottom*) are given. Optical components used in set up include a polarizing cube (C), a half-wave plate (WP), lenses (L), and reflectors (R). Diagnostic components include programmable delay generators (PDG) and an intensified CCD camera (ICCD). (BD corresponds to the beam dump)

focused with a 40 cm and 75 cm plano-convex BK7 focusing lenses, which were moved along the laser beam path to vary the laser spot size. Likewise, the CO<sub>2</sub> laser was focused using a 40 cm plano-convex ZnSe lens, moved to different positions for changing the spot size. Two delay generators were used for controlling the timing sequence between the pump and reheating laser. Though all the experiments were performed as single shots, the YAG laser flash lamps were

operated at 10 Hz to overcome the laser beam expansion caused by thermal lensing.

The plasma emissions were analyzed in the optical region using a 0.5 m Czerny-Turner spectrograph. A 40 cm lens focused the light emitted from the plasma plume into a 3 mm high entrance slit of the spectrograph operating within a 250–800 nm spectral window. The focusing lens was mounted to a dove-tail translation base, to allow the evaluation of the plasma at different points during its expansion. Most spectra were recorded with a 600 grooves/mm, but 150 grooves/mm and 1800 grooves/mm were used to record spectra when determining electron temperature and densities, respectively. An intensified charged couple device (ICCD) detector was used for collecting the dispersed light signal. The ICCD is synchronized with lasers using a programmable delay generator (PDG) with a jitter of  $\pm 1$  ns.

### 3 Results

The LIBS technique often concentrates on the ‘delayed’ atomic emission region for obtaining a better signal-to-noise ratio by discriminating continuum emission [10]. In the LIBS ‘regime’, the temperature will drop to  $\sim 1\text{--}2$  eV and the density will be at least one to two orders lower compared to the earliest time of plasma creation. In this regime, most of the emission is due to lowly charged ions ( $Z \leq 1$ ) and excited neutrals, and hence, this plasma region emits light in the visible region. We utilized optical emission spectroscopy (OES) diagnostics to characterize the light emission from the plasma region in both early and later times. The time gating ability of the ICCD helps to discriminate the LIBS emission from the strong continuum from the plasma. LIBS experiments were done in atmospheric pressure, and hence, the plume generated by the laser was severely confined to the target surface. A typical LIBS plume length under these conditions was 3 mm. Plasmas were evaluated at a point 2 mm from the target surface, to avoid the intense, broadband continuum emissions that exist close to ( $< 1$  mm) the target surface.

In a DP-LIBS system, spectral enhancements directly depend on the delay between pulses, the laser spot sizes, and the pre-pulse energy. It was discovered that a dual-pulse plasma will always provide some degree of enhancement, regardless of the parameters selected, and the resulting spectra of a CO<sub>2</sub>-reheated YAG plasma is always more intense than the sum of its components. Figure 2 gives typical spectra of 50 mJ YAG laser plasmas, of 400 mJ CO<sub>2</sub> laser plasmas, and a combination of both with an inter-pulse delay of 600 ns. The delay and gate width used for detection were 300 ns after the peak of the laser pulse and 3  $\mu$ s respectively. In the reheating case, the gate delay was set at 300 ns after the peak of the YAG laser pulse. The prominent lines in

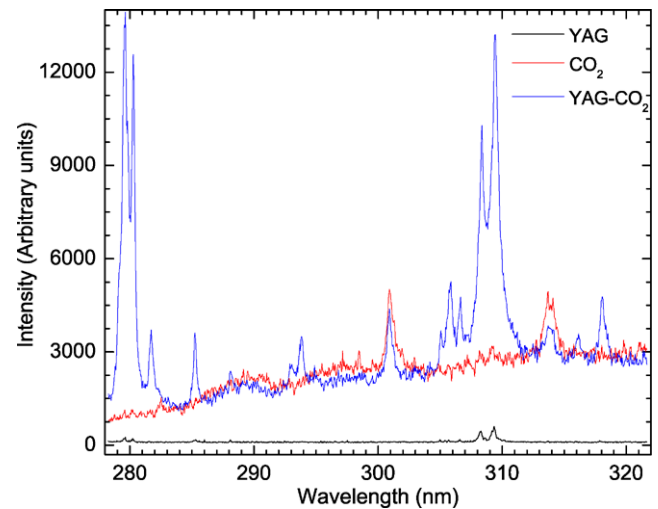


**Fig. 2** Typical 3  $\mu$ s gated spectra of YAG, CO<sub>2</sub>, and CO<sub>2</sub>-reheated Al plasmas. 50 mJ, 1.064  $\mu$ m YAG pulses focused to a  $\sim 1.13$  mm diameter spot size, along with 400 mJ, 10.6  $\mu$ m CO<sub>2</sub> pulses focused to a 4 mm spot size were used in these trials. The prominent multiplet near 280 nm consists of Mg II lines, caused by Mg impurities

Fig. 2 are an Al doublet at 308.2 nm and 309.3 nm, Al<sup>+</sup> at 281 nm and a Mg<sup>+</sup> multiplet at 280 nm. The origin of Mg lines in the spectra is due to presence of Mg impurities in the Al target. From the figure it is clear that the enhancement factor for various lines are different, and that ionic lines showed maximum enhancement.

#### 3.1 Inter-pulse delay variation

The delay between the LIBS plume generation laser and the reheating laser is one of the main parameters that affects the signal enhancement in DP-LIBS.

For each inter-pulse delay 20 sequential images were recorded with a 3  $\mu$ s gate time. The first spectrum was recorded 200 ns after the peak of the YAG laser pulse, and the subsequent spectra were delayed by 300 ns from the preceding one.

A slit width of 10  $\mu$ m was used for spectrograph throughout all experiments. In this experiment, Al plasmas were created with a 1.064  $\mu$ m, 50 mJ, YAG laser pre-pulses focused to a 0.8 mm spot size. The delay generator settings were then altered to reheat the pre-plasma plume with a 400 mJ CO<sub>2</sub> laser pulse with a 5 mm spot-size at various pre-determined times, and were recorded with a 3  $\mu$ s gate time.

The maximum signal enhancement noticed for Al neutral and Al ionic lines are given in Fig. 3. The signal enhancement was found to be strongly dependent on the inter-pulse delay throughout the plasma’s entire expansion, as seen in Fig. 3. The greatest enhancement was found to occur when the CO<sub>2</sub> reheats the plasma 750 ns after the pre-pulse. With a 750 ns inter-pulse delay, a 100 $\times$  enhancement is noticed for ionic lines. However, the enhancement factor for

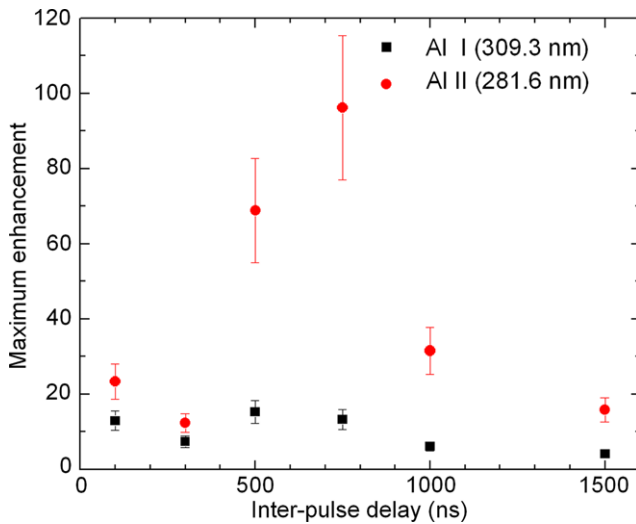


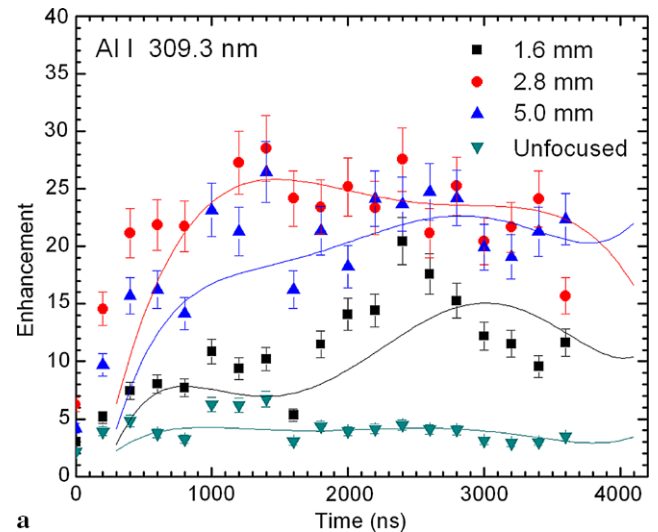
**Fig. 3** The effects of different YAG-CO<sub>2</sub> pulse delay times on the enhancement of neutral and ionized Al spectra. Al plasmas were created with a 50 mJ, YAG laser pre-pulses focused to a 0.8 mm spot size, reheated with a 5 mm 400 mJ CO<sub>2</sub> laser pulse at various pre-determined times, recorded with a 3  $\mu$ s camera gate time

neutral lines is considerably lower (5–15 $\times$ ), and showed a fluctuation with inter-pulse delay.

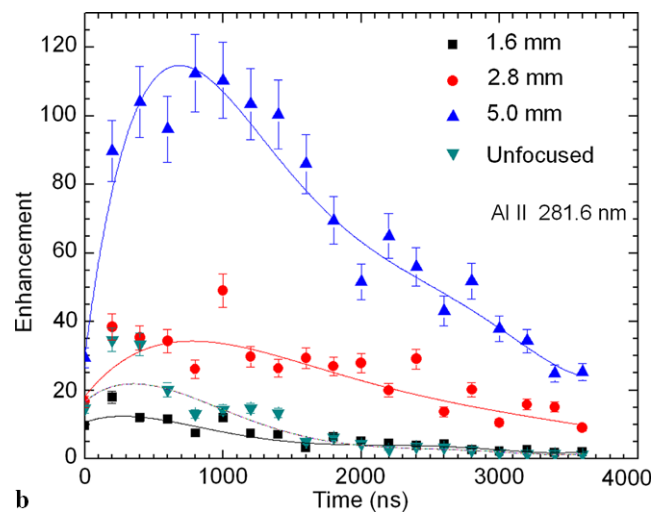
### 3.2 CO<sub>2</sub> laser spot size variation

Effective coupling between the pre-plume and the reheating pulse is essential for obtaining the highest signal enhancement in DP-LIBS. Hence, we changed the 10.6  $\mu$ m laser spot size to monitor the efficient coupling of the reheating with the LIBS plume. In this experiment, laser plasmas were created with 1.06  $\mu$ m, 50 mJ YAG laser pre-pulses to a  $\sim$ 1.13 mm diameter, and were reheated with a 10.6  $\mu$ m; 400 mJ CO<sub>2</sub> laser pulse. A 40 cm ZnSe lens was placed at various points along the beam path to alter the CO<sub>2</sub> spot diameter. For each of these plasmas, we maintained an inter-pulse delay time of 600 ns and recorded 20 sequential spectra with a 3  $\mu$ s gate time. The first spectrum was recorded 200 ns after the peak of the YAG laser pulse, and each successive spectrum was then delayed 300 ns from the previous spectrum.

Figure 4 clearly shows that CO<sub>2</sub> beam focusing is absolutely crucial to signal enhancement, but the degree of focusing required is entirely dependent on which spectral lines are to be excited. Atomic Al lines demonstrate similar enhancement with 3–5 mm CO<sub>2</sub> beam diameters, while ionic lines respond better to larger (5 mm) spot sizes. Furthermore, the atomic and ionic peak enhancements occur at different times, with the atomic lines peaking at  $\sim$ 1  $\mu$ s, while the ionic lines peak at  $\sim$ 650 ns. The neutral line enhancement was also shown to exhibit oscillatory behavior. Even when an unfocused CO<sub>2</sub> beam is used for reheating, we no-



**a**



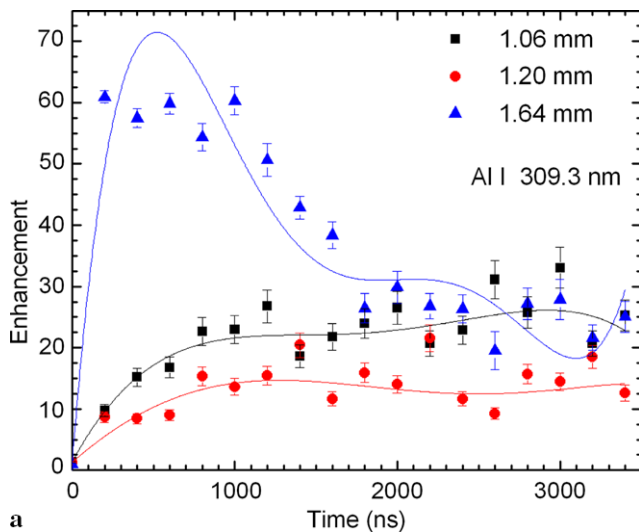
**b**

**Fig. 4** The effects of different CO<sub>2</sub> spot size variation on the enhancement of (a) neutral and (b) ionized Al spectra as a function of time with respect to the reheating pulse. These plasmas were generated with 1.06  $\mu$ m, 50 mJ YAG laser pre-pulses focused to a  $\sim$ 1.13 mm diameter, and were reheated with a 10.6  $\mu$ m; 400 mJ CO<sub>2</sub> laser pulse, and focused with a 40 cm ZnSe lens. There was an inter-pulse delay time of 600 ns. These plots were created from 20 sequential spectra recorded with a 3  $\mu$ s gate time. The first spectrum was recorded 200 ns after the peak of the YAG laser pulse, and each successive spectrum was then delayed 300 ns from the previous spectrum

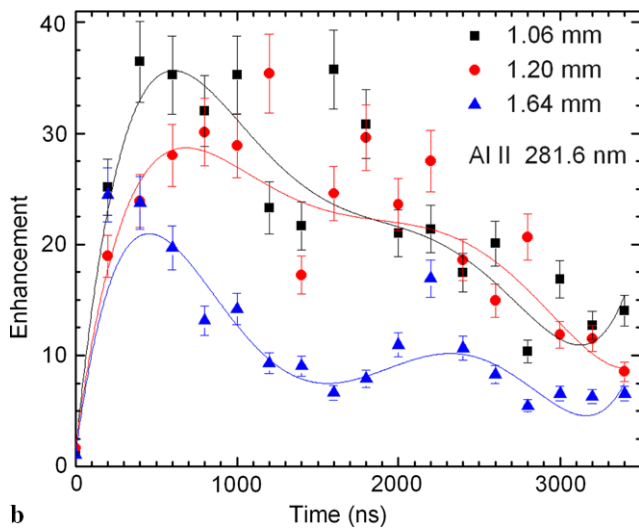
ticed a signal enhancement of 5–20 $\times$ , which is significantly greater than some YAG-YAG DP-LIBS schemes [21].

### 3.3 YAG laser spot size variation

The pre-plasma laser beam spot size determines the power density at the target surface, which is directly related to the material ablation, and hence, the LIBS signal intensity. The change in the spot size is also related to the expansion dynamics of the plume, and hence, it will affect the coupling of reheating beam. For these reasons, we varied the pre-plume spot size while keeping the same pulse energy. A 1.064  $\mu$ m,



a



b

**Fig. 5** The effects of different YAG spot size variation on the enhancement of (a) neutral and (b) ionized Al spectra as a function of time with respect to the reheating pulse. A 1.064  $\mu\text{m}$ , 50 mJ YAG laser was focused for creating Al plasmas and was reheated with a 10.6  $\mu\text{m}$ ,  $\sim 400$  mJ  $\text{CO}_2$  laser pulse, focused to a 2.8 mm diameter. The inter-pulse delay was set at 600 ns. 20 sequential spectra were recorded with a 3  $\mu\text{s}$  gate time. The first spectrum was recorded 200 ns after the peak of the YAG laser pulse, and each successive spectrum was then delayed 300 ns from the previous spectrum

50 mJ YAG laser was focused with a 40 cm lens to various beam diameters, creating small Al plasmas which were then immediately reheated with a 10.6  $\mu\text{m}$ , 400 mJ  $\text{CO}_2$  laser pulse, focused to a 2.8 mm diameter with a 40 cm ZnSe lens. There was a delay of 600 ns between both pulses. Another 20 sequential spectra were recorded with a 3  $\mu\text{s}$  gate time. The first spectrum was recorded 200 ns after the peak of the YAG laser pulse, and each successive spectrum was again delayed 300 ns from the previous spectrum.

The YAG spot size was shown to strongly affect the signal enhancement, as shown in Fig. 5, but the magnitude of

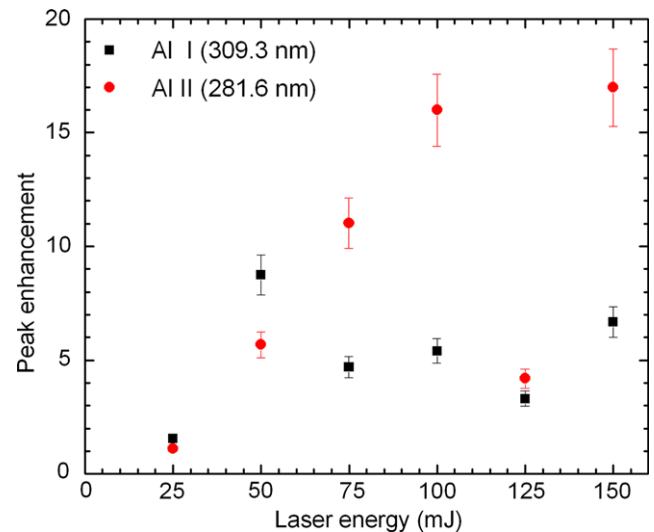


**Fig. 6** The effects of different YAG laser energy variation on the enhancement on neutral and ionized Al spectra. A YAG pre-plasma laser spot was maintained at a consistent 0.8 mm diameter while a 1 cm diameter, unfocused  $\text{CO}_2$  laser pulse (400 mJ) reheats the plasma. The inter-pulse delay was set to 600 ns and was recorded with a 3  $\mu\text{s}$  gate time

that enhancement varies among different transitions—ionic transitions see better enhancement from tightly focused pre-pulse beams, while atomic lines require a larger spot size. Preliminary studies with highly focused YAG pre-pulses ( $\leq 300 \mu\text{m}$ ) showed little or no signal enhancement, due to the small amount of material ablated by the pre-pulse. The enhancement is prone to time-dependent oscillations, but in all cases it peaks  $\sim 450$ – $600$  ns after the reheating pulse.

### 3.4 YAG energy variation

The intensity of the pre-plasma laser pulse affects the characteristics of LIBS plume, as well as material ablation. Typically for ns laser plumes, the leading edge of the laser pulse generates plasma above the target surface, and the remaining laser pulse energy will be used for heating the plasma, rather than interacting with the target surface. For this experiment, a YAG pre-plasma laser spot was maintained at a consistent 0.8 mm diameter while a 1 cm diameter, unfocused  $\text{CO}_2$  laser pulse (400 mJ) was used for reheating. The enhancements in both the excited neutral and ionic lines were measured with an inter-pulse of 600 ns, the results of which are shown in Fig. 6.

From this, it was learned that ionic line signal enhancement directly depends on pre-pulse laser energy, but the atomic lines see an optimum enhancement at  $\sim 50$  mJ, and that increasing the pre-pulse energy to  $> 75$  mJ does not have an effect on atomic line emission intensity. Likewise, the ionic lines also demonstrate a saturating trend. This is because laser pulses can only ablate and excite a finite amount of material to a plasma state; this plasma then shields the

target from further ablation, and the remainder of the beam is spent reheating the plasma shield. For this reason, the energy of the YAG pre-pulses in a DP-LIBS system should be <100 mJ, as higher energies will fail to ablate any additional material and will decrease the overall wall-plug efficiency of the system.

#### 4 Discussion

Our results indicate that the sensitivity of LIBS can be significantly improved with the use of IR lasers for reheating the initial plasma. However, the enhancements of the signal depend on several experimental parameters, and the enhancement factor is different for neutral and ionic lines. In the present experiments, the maximum enhancement was noticed for ionic lines. The reheating pulse spot size effect showed a considerable enhancement in signal intensity, even with a minimum interaction between the pre-LIBS plasma and the reheating beam. For example, we found enhancement factors of 5 and 20 for neutral and ionic lines, respectively, where the interaction between the pre-plasma and reheating beam is minimum (the plasma size is ~3 mm and the reheating beam is 1 cm in diameter). This enhancement factor is still higher than the results of traditional YAG-YAG DP-LIBS. This shows the importance of using long wavelength lasers for reheating in DP-LIBS.

Experimental studies with various parameters of dual-pulsed plasmas displayed some spectral enhancement when compared to single-pulse plasmas created under the exact same conditions. The optimum inter-pulse delay time, with respect to pre-pulse peak time, was found to be 500–750 ns. Laser spot sizes profoundly affect signal enhancement, to a degree determined by which species are being excited. Atomic lines were optimized with a 50 mJ, ~1.64 mm diameter pre-pulse and reheated with a 3–5 mm CO<sub>2</sub> beam diameter, while ionic lines best responded to a larger reheating pulse (5 mm). Highly focused YAG pre-pulses (~300 μm) will produce a negligible enhancement, due to the low mass ablated by the reduced pre-pulse. Plasma shielding causes a saturating trend with pre-pulse energy variation, starting at 50 mJ for atomic lines and 100 mJ for ions. The enhancement is prone to time-dependent oscillations, peaking ~1 μs after pre-plasma formation. The oscillations are possibly due to the time-dependent intensity fluctuations of the reheating pulse (see Fig. 1).

The signal enhancement in the DP-LIBS can be due to several mechanisms, and the relative importance of each is still subject to discussion. In order to get better information, we estimated the temperature and density of the pre-LIBS and reheated LIBS plasmas using time-resolved OES recorded at a single fixed point 2 mm from the target surface. For density and temperature measurements, plasmas

were created with a 1.064 μm, 50 mJ YAG laser pulse focused to a ~1 mm diameter, and were re-heated with CO<sub>2</sub> laser pulses focused to a 5 mm diameter, with an inter-pulse delay time of 750 ns. The OES electron temperature and density measurements recorded with a 20 ns gate time. The electron density was estimated from the Stark broadening of its line emission under similar experimental conditions (pre-pulse alone and reheating). This is determined by fitting Lorentzian functions to transition peaks and calculating their full-widths at half maximum (FWHM) [22–24]. Because of the lack of intense lines in pre-plume, Al neutral line at 396.2 nm was selected, and self-absorption was evident in our spectral data in the earliest times during reheating. The results of this experiment showed that there is no significant difference between the electron densities of single-pulse and dual-pulsed Al plasmas. In both cases, the density starts out at ~10<sup>18</sup> cm<sup>-3</sup>, and rapidly drops to about 1.75 × 10<sup>17</sup> cm<sup>-3</sup> within 300 ns after the pre-pulse plasma formation.

Electron temperatures were determined through the Boltzmann plot method, evaluating the Al I doublets located at 308.2 nm, 309.3 nm, and at 393.5 nm, 396.2 nm. YAG laser-produced pre-plasmas were observed to have an initial temperature of 1.5 eV, which then dropped rapidly to a consistent 0.5 eV after 0.5 μs. The CO<sub>2</sub>-reheated YAG plasmas begin much the same way, but see a rapid increase in electron temperature, peaking at ~2.5 eV during reheating at ~1 μs then dropping off to a consistent ~1 eV after 2 μs. From this, it is evident that the CO<sub>2</sub> laser pulse efficiently reheats the pre-plasma. This reheating is likely achieved through inverse Bremsstrahlung.

The density estimate showed that there are negligible changes in the reheated plume compared to pre-LIBS plume, while the temperature measurement showed a significant rise. The major laser absorption mechanism in a laser-ablated plume is inverse Bremsstrahlung. The rate of inverse Bremsstrahlung absorption is approximated by the following relation [25]:

$$a_{ib}(\text{cm}^{-1}) = 1.37 \times 10^{-35} \lambda^3 n_e^2 T_e^{-\frac{1}{2}} \quad (1)$$

where  $n_e$  is the electron density (in cm<sup>-3</sup>),  $T_e$  is the electron temperature (in K), and  $\lambda$  is the wavelength of the light being absorbed (in μm). Inverse Bremsstrahlung is a strongly wavelength dependent process. Hence, the selection of wavelengths for the pre-pulse ( $\lambda_{\text{pre-pulse}}$ ) and reheating pulse ( $\lambda_{\text{reheating}}$ ) has been shown to profoundly affect the enhancement, with the  $\lambda_{\text{reheating}} > \lambda_{\text{pre-pulse}}$  case yielding a much greater enhancement than trials employing a  $\lambda_{\text{reheating}} < \lambda_{\text{pre-pulse}}$  scheme. In an ideal scenario, UV lasers are to be used for pre-plasma generation, because their shorter wavelengths offer greater mass ablation with less plasma shielding [17, 26]. Based on the density and temperature measurements of pre-plasmas, the inverse absorption

length was calculated from Eq. (1) to determine the effectiveness of the inverse Bremsstrahlung absorption process. The inverse Bremsstrahlung absorption length for a CO<sub>2</sub> laser reheating scheme was found to be 3.86 cm<sup>-1</sup>. This allows for the reheating of the entire plasma volume, greatly enhancing its light emission as compared to a YAG pulse absorbed by an identical pre-plasma, which would have an absorption length three orders lower.

Our findings show that there is a significant variation between the temperatures and inverse absorption lengths of single- and dual-pulse plasmas. This would indicate that inverse Bremsstrahlung is the dominant process, as opposed to the shockwave-induced coupling model [8, 9]. Our spectral studies showed significant variation in enhancement factor for various lines studied. For example, the Mg II multiplet from 279–280 nm showed an enhancement factor of more than 1000×. This is because the Mg II lines in the spectra are resonance lines, which see a preferential excitation from the ground state, as opposed to the Al II transition at 281.6 nm, which has a lower energy level of 7.43 eV [27]. Likewise, recent studies [5, 28] shows that an entirely different set of parameters are necessary to optimize the emissions from C and Ag.

## 5 Summary

We investigated DP-LIBS experimental scheme with a YAG-CO<sub>2</sub> laser combination. The study of the role of the spot sizes, inter-pulse delay times, energies of the preheating and reheating pulses in the LIBS sensitivity improvements has been carried out. Our results showed that an IR laser pulse reheating will always cause some enhancement, regardless of the conditions. The magnitude of this enhancement was found to be a function of a number of laser parameters, such as laser energy, wavelength, spot size, the time between pulses, etc. The enhancement factor is found to be dependent on the energy levels of the lines, and resonance lines provided maximum enhancement. For example, the resonance lines of Mg ions showed an enhancement factor of more than 1000. Compared to excited neutral lines, ionic lines always showed higher enhancement. Our results indicate that considerable improvement in sensitivity is possible even with an unfocused reheating beam.

Optical emission spectroscopic studies showed there is negligible difference in the electron densities of single-LIBS and reheated LIBS plume. However, the temperature measurement showed a considerable increase due to reheating. Hence the improved sensitivity with a YAG-CO<sub>2</sub> laser combination is due to effective reheating of the preplume with a longer wavelength laser due to efficient inverse Bremsstrahlung absorption.

The differences in the signal enhancement between the Mg and Al transition lines clearly shows that the DP signal

enhancement varies between transitions, though the nature of this variation, along with any Z-dependence or effect of the target material's electron configuration has yet to be determined. An earlier study has shown that 266 nm pre-pulses offers an improved mass ablation rate that yields comparable results in spite of the power loss involved with fourth-harmonic generation [26]. Hence, UV pre-pulses could possibly increase the signal enhancement, allowing for greater stand-off ranges in remote detection applications to ensure safety to personnel involved hazardous material detection and security applications.

**Acknowledgements** This work was supported by the Department of Energy National Nuclear Security Administration under Award number DE-NA0001174.

## References

1. J. Singh, S. Thakur, *Laser-Induced Breakdown Spectroscopy* (Elsevier Science, Amsterdam, 2007)
2. A. Ford, R. Waterbury, J. Rose, K. Pohl, M. Eisterhold, T. Thorn, K. Lee, E. Dottery, Proc. SPIE **7665**, 76650Y (2010)
3. A. Bol'shakov, J. Yoo, C. Liu, J. Plumer, R. Russo, Appl. Opt. **49**, C132 (2009)
4. D. Killinger, S. Allen, R. Waterbury, C. Stefano, E.L. Dottery, Opt. Express **15**, 12905 (2007)
5. B. Rashind, R. Ahmed, R. Ali, M.A. Baig, Phys. Plasmas **18**, 073301 (2011)
6. P. Benedetti, G. Cristoforetti, S. Legnaioli, V. Palleschi, L. Pardini, A. Salvetti, E. Tognoni, Spectrochim. Acta, Part B **60**, 1392 (2005)
7. G. Cristoforetti, S. Legnaioli, V. Palleschi, A. Salvetti, E. Tognoni, Appl. Phys. B **80**, 559 (2005)
8. R. Noll, R. Sattmann, V. Sturm, S. Winkelmann, J. Anal. At. Spectrom. **19**, 419 (2004)
9. L. St-Onge, V. Detalle, M. Sabsabi, Spectrochim. Acta, Part B **57**, 121 (2002)
10. J. Uebbing, J. Brust, W. Sdorra, F. Leis, K. Niemax, Appl. Spectrosc. **45**, 1419 (1991)
11. A. Bogaerts, Z.Y. Chen, R. Gijbels, A. Vertes, Spectrochim. Acta, Part B **58**, 1867 (2003)
12. X. Pu, N. Cheung, Appl. Spectrosc. **57**, 588 (2003)
13. X. Pu, W. Ma, N. Cheung, Appl. Phys. Lett. **83**, 3416 (2003)
14. S. Lui, N. Cheung, Anal. Chem. **77**, 2617 (2005)
15. M. Corsi, G. Cristoforetti, M. Giuffrida, M. Hidalgo, S. Legnaioli, V. Palleschi, A. Salvetti, E. Tognoni, C. Vallebona, Spectrochim. Acta, Part B **59**, 723 (2004)
16. L. Cabalin, J. Laserna, Spectrochim. Acta, Part B **53**, 723 (1998)
17. R. Russo, X. Mao, O. Borisov, H. Liu, J. Anal. At. Spectrom. **15**, 1115 (2000)
18. X. Mao, W. Chan, M. Shannon, R. Russo, J. Appl. Phys. **74**, 4915 (1993)
19. X. Mao, W. Chan, M. Caetano, M. Shannon, R. Russo, Appl. Surf. Sci. **96**, 126 (1996)
20. J. Aguilera, C. Aragon, F. Penalba, Appl. Surf. Sci. **127**, 309 (1998)
21. K. Eland, D. Stratis, J. Carter, S. Angel, Proc. SPIE **3853**, 288 (1999)
22. S. Harilal, B. O'Shay, M. Tillack, M. Mathew, J. Appl. Phys. **98**, 013306 (2005)
23. H. Griem, *Spectral Line Broadening by Plasmas* (Academic Press, New York, 1974)

24. N. Konjevic, A. Lesage, J.R. Fuhr, W.L. Wiese, *J. Phys. Chem. Ref. Data* **31**, 819 (2002)
25. J. Chang, B. Warner, *Appl. Phys. Lett.* **69**, 473 (1996)
26. R. Waterbury, A. Pal, D. Killinger, J. Rose, E. Dottery, G. Ontai, *Proc. SPIE* **6954**, 95409 (2008)
27. Y. Ralchenko, A. Kramida, J. Reader, NIST ASD Team, NIST atomic spectra database (ver. 4.0.1) (Online). National Institute of Standards and Technology, Gaithersburg, MD (2010)
28. M. Asgill, M. Brown, K. Frische, W. Roquemore, D. Hahn, *Appl. Opt.* **49**, C110 (2010)